Acta Geotechnica (2013) 8:215–221
DOI 10.1007/s11440-012-0184-5

SHORT COMMUNICATION

Formation of drying crack patterns in soils: a deterministic approach

Hervé Peron · Lyesse Laloui · Liang-Bo Hu · Tomasz Hueckel

Received: 3 February 2012 / Accepted: 20 July 2012 / Published online: 19 August 2012

Abstract Soils, as well as most of deformable multiphase porous materials, are likely to suffer from desiccation cracking, leading to the formation of regular crack patterns affecting their permeability. The ensuing crack spacing has often been related to a concept sometimes called "sequential infilling": it is assumed that desiccation cracks are formed by successive generations. However, such a concept does not consider the pattern of a simultaneous crack formation at a given moment. Using our desiccation cracking test results and their numerical simulation, we propose a consistent explanation for the formation of desiccation crack patterns in soils. We show that the "sequential infilling" concept is suitable only when the position of the crack(s) clearly stems from the stress field. To derive an estimate of the desiccation crack spacing, the overall energy of the system needs to be considered. Statistical variability should be superimposed on the mean deterministic conditions discussed here.

Keywords Crack · Desiccation · Drying · Experimental testing · Soil

H. Peron · L. Laloui (✉)
Laboratory of Soil Mechanics, Ecole Polytechnique Fédérale de Lausanne, Station 18, 1015 Lausanne, Switzerland
e-mail: lyesse.laloui@epfl.ch

L.-B. Hu
Department of Civil Engineering,
University of Toledo, Toledo, OH 43606, USA

T. Hueckel
Department of Civil and Environmental Engineering,
Duke University, Durham, NC 27708, USA

1 Introduction

In soil science, desiccation cracks are of interest as they have an impact on transport of gases, moisture and nutrients to the plant roots [11]; in geological analyses, they indicate an air exposure of sediments [28]. Desiccation cracking alters the bearing capacity and overall stability of foundation ground, dams and many earthen structures [21], as well as the permeability of soil barriers for waste confining [1]. Desiccation cracking primarily affects the hydro-mechanical properties of soils, especially their strength, compressibility and permeability. With this respect, the critical parameters are crack spacing and crack connectivity, the former being focused on here.

Evaporation of the wetting liquid (generally water) from a deformable porous medium (here soil) induces drying shrinkage. Desiccation cracks are likely to occur if the shrinkage is constrained and if tensile stresses are generated in the material, which reaches its tensile strength [8, 10, 12, 19, 21, 25]. Typically, these constraints may arise from a frictional or any other traction or displacement boundary conditions. Moreover, any eigenstress concentrations caused by a drying-induced water content heterogeneity, and intrinsic factors such as texture (existence of large particles, [31]) or a soil micro-structure (solid network, [29]) may form such constraints.

2 Experimental characterization

Figure 1 shows an example of desiccation crack pattern in a mud with remarkably uniform crack spacing. Desiccation crack patterns are commonly two dimensional. However, for the sake of simplicity, it is convenient to first quantify the process in one dimension [22]. In order to identify the

Fig. 1 Example of desiccation cracks in dry mud, North Panamint Playa, Death Valley National Park, USA

mechanisms that lead to such a well-defined crack spacing, we have chosen to study the desiccation of rectangular mud bars (length, L, 300 mm; width, l, 50 mm; height, h, 12 mm) made up of initially water-saturated remoulded clayey soil. The clay mineral content of the soil is 25 % (illite, smectite and chlorite); the remaining part is essentially made up of quartz, calcite and feldspar. The soil contains no particles greater than 0.09 mm. The soil is classified as "inorganic clay of medium plasticity", using the Swiss SN 670008a standard, which is adapted from the International Unified Soil Classification System chart.

For the tests, the dry powder of soil was mixed with deaired and demineralized water at gravimetric water content of about 48 %. The resulting slurry was then vigorously mixed and vibrated for 2 min to remove air bubbles. Such a preparation guaranties an initially saturated state. After being prepared and before use, the slurry was left to settle for at least one day to ensure homogenization. This preparation prevents formation of any initial soil structure such as particle aggregates.

The shrinkage of the bar has intentionally been impeded at the base in the axial direction only, Fig. 2d, e, using a metallic substrate with thin, 2-mm spaced and parallel, sharp notches. The evolution of gravimetric water content w (%) has been monitored. A total of 17 bars have been air-dried. All of the tests have been performed in a climate chamber with controlled relative humidity of 40 ± 4 % (absolute variation) and temperature fixed at 19 ± 1 °C.

Time evolution of the sample mass was recorded with a balance, by continuous weighing of the bar of drying soil lying on the metallic support. Gravimetric water content was finally deduced, knowing the dry mass of the sample, obtained thanks to oven drying of the sample after air-drying completion.

After about 17-h drying, a regular pattern of 6 cracks (4 bars out of 17), 7 cracks (12 of 17) or 8 cracks (1 of 17) has appeared always in the direction perpendicular to the direction of the axial restraint (Fig. 2d, e). Considering the average value of seven cracks, the mean crack spacing at the moment when cracking ended was 4.1 cm. The configuration of crack spacing (for the bars exhibiting seven cracks) is shown in Fig. 2d, e. Before the parallel cracks appeared, a slight detachment of the specimen from the base occurred at the two bottom corners. The entire process of formation of the observed crack pattern lasted a relatively limited amount of time, about 1.5–2 h. The water content during the whole process of cracking varied between value of $w = 25.5$ % (maximum average measured value when the first crack appeared) and $w = 21.5$ % (minimum measured value when the last crack appeared. The average water content across the bar decreased along the process, as the new cracks were appearing, but not after the third crack (Fig. 2d). Local water content was traced at the sites of cracks, sampled immediately after a crack would appear. As seen in Fig. 2d, the water content at the moment of cracking does not vary much, almost independently of which in order of appearance a given crack is. During this time period, the majority of cracks clearly formed following the sequential infilling scenario, except that not necessarily exactly halfway between two existing cracks of the previous generation. However, in an appreciable number of cases, cracks could appear simultaneously (either initial cracks or subsequent cracks between two adjacent pre-existing cracks), therefore deviating from the sequential model.

3 Modelling

To further quantify the processes, we investigate the stress field arising from the desiccation using a finite element simulation. We adopt a total stress approach within the framework of Biot theory of porous media; an effective stress approach is adopted in our study on the meso-scale criterion for an individual crack onset [13–15, 26, 27]. In particular, we take advantage of "thermo-elastic analogy", that is, the analogy between the equation describing moisture transport and the elastic response to changes in water content, on the one hand, and the thermo-elasticity of the heat diffusing elastic medium, on the other hand (see e.g. [18]). According to Biot theory approach, a relation is established between total stress, strain and an additional variable like (fluid) mass change(s) or pore pressure(s) (see e.g. [9]). When the latter component is small, the "regular" total stress approach is recovered. In this sense any limit criterion, strength or yield limit, should in principle encompass such "additional" variable, unless there is an experimental evidence of a negligible effect. With such a formulation, drying-induced stress field arising from both mechanical boundary conditions and water content heterogeneities is computed. Alternatively, strains are viewed as a combination of a drying shrinkage–induced (volumetric) part, ε^h, proportional to water content change Δw, and a mechanical part, ε_{ij}^{me}, generated to satisfy strain compatibility requirement. The mechanical strain is linearly related to the total stress via a constant elastic stiffness tensor,

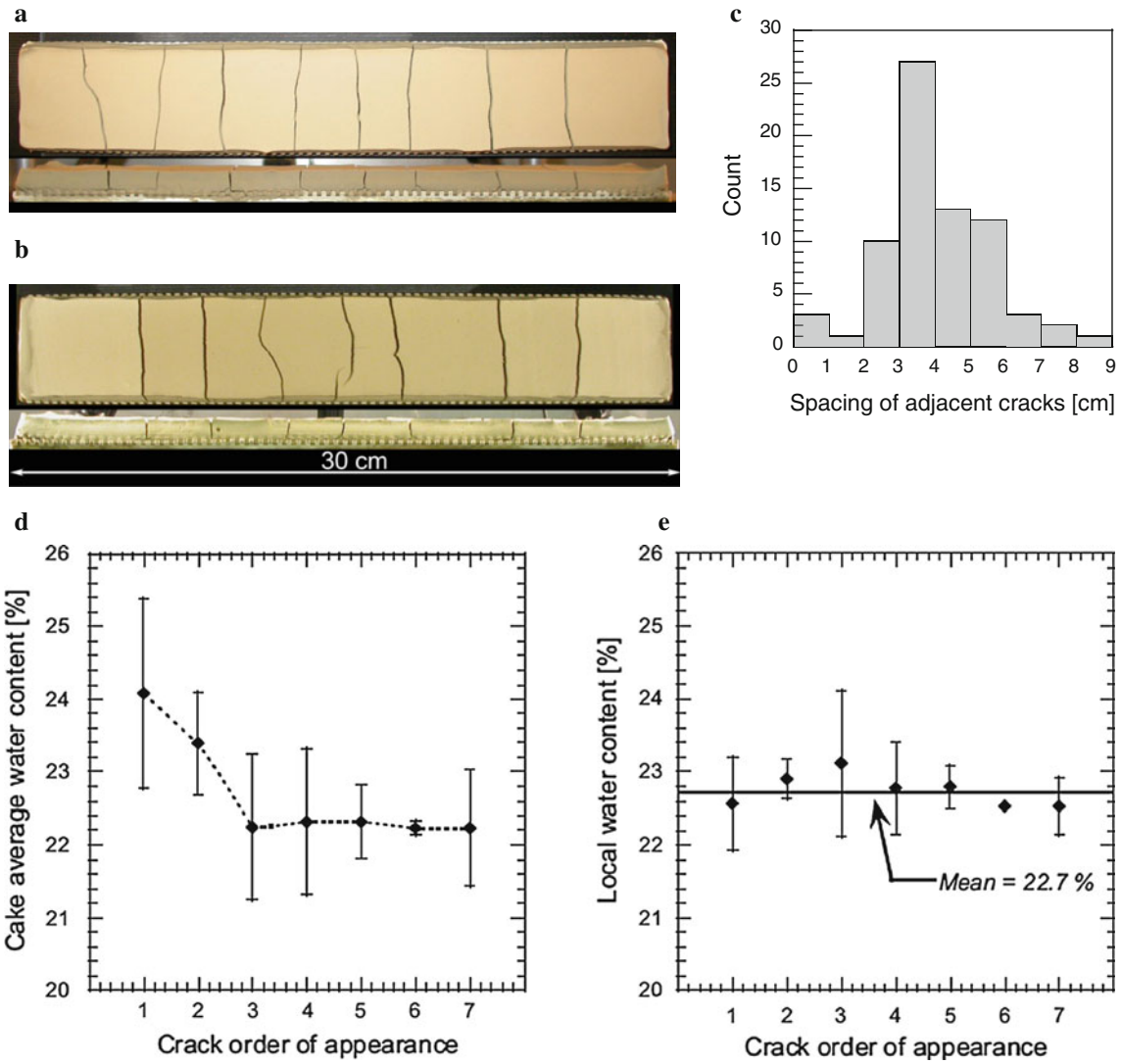

Fig. 2 Experimental desiccation crack patterns. **a** Final crack pattern with height fractures, top view (*upper* picture) and side view (*lower* picture). **b** Final crack pattern with seven fractures, top view (*upper* picture) and side view (*lower* picture). **c** Repartition of crack spacing values for the bars with seven cracks. **d** Average water content at the moment of appearance of subsequent cracks. **e** Local water content in the vicinity of each crack versus crack order of appearance

D_{ijkl}. Therefore, in terms of the total stress and the strain tensors, respectively, σ_{ij} and ε_{kl}, the following relationship holds: $\sigma_{ij} = D_{ijkl}\varepsilon_{kl} + B_{ij}\Delta w$ where $B_{ij} = -\alpha D_{ijkl}\delta_{kl}$, where δ_{kl} is the Kronecker symbol. α is a shrinkage strain coefficient. However, it needs to be kept in mind that the strain induced by (at least first cycle of) drying is largely inelastic, hence irreversible [24].

Biot theory comprises another (scalar) relationship between the evolution of the water content, *w,* and volumetric strain and pore pressure. In our case we consider only changes of water content as a result of diffusion and its gradients governed by a diffusion-like equation, neglecting other effects, including body sinks due to internal evaporation. Indeed, evaporation is simulated via prescribed water flux at the external surfaces through appropriate boundary conditions. Stress and strains are taken as positive in compression.

A 2D model of the bar used in desiccation tests has been examined (Fig. 3). The bar (plain strain hypothesis) has been subjected to a condition of zero displacement in the axial direction at the bottom. Drying boundary conditions consist in imposing decreasing water content values on the surfaces of the top and sides of the bar, with a constant rate of 1.2 % per hour (as recorded during the experiments). The simulation has been performed with the finite element code GefDyn [2]. In the simulation $\alpha = 1.26 \times 10^{-2}$ (calculated from shrinkage experiments), $E = 1 \times 10^5$ Pa (arbitrary value, its value scales the order of magnitude of

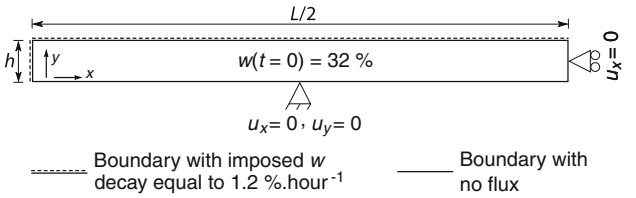

Fig. 3 Finite element model with initial and boundary conditions. u_x and u_y are the horizontal and vertical displacements, respectively, w is the gravimetric water content, t is the time, L is the length of the bar, h its height

the stress field, but not the distribution of the stresses) and $v = 0.3$ (value known for the simulated material), E and v enter the elastic stiffness tensor D_{ijkl}.

The advantage of using the total stress via Biot theory is in the possibility of obtaining simple energy equations, and linear fracture mechanics concepts, as total stress during desiccation results to be tensile, as opposed to the compressive effective stress, due to significant values of suction.

Results (Fig. 4a, b) show that maximum tensile stress (in absolute value) in horizontal direction is reached in the middle of the bar length, indicating that the first vertical crack would initiate at this location. Linear fracture mechanics is a convenient tool to study the conditions for desiccation crack pattern formation from an estimate of the total stress field [21, 25]. In the conditions of the simulation, linear fracture mechanics shows that a desiccation crack is unstable [3, 5] and hence should propagate across the specimen thickness. As a consequence, the stress in the sample is expected to react to stress boundary condition change, generally speaking, by producing a partial unloading. Subsequently, as evaporation progresses, the loading process is resumed, eventually leading to a crack formation in the two newly created parts of the original sample. This finally results in formation of a regular crack spacing. This is the "sequential infilling" scenario (see e.g. [6]). Independently from the above scenario, the core of the bar is usually slightly wetter than the top surface (according to experimental observations), causing a small tensile stress concentration at the bar top surface (Fig. 4). The slight detachment experimentally observed near the sample bottom is explained by a shear effect. It induces large but localized tensile stresses, generating conditions for early crack formation. The complex stress field in this zone impedes a further crack extension.

4 Interpretation and discussion

The simulations reveal that minor principal stress (tensile) is rather uniformly distributed in the central region of the bar. Eventually, if the specimen is sufficiently long, the tensile stress field is likely to be nearly constant, at least along surfaces parallel to the external drying surface. Therefore, the concept of sequential infilling fails to explain the formation of regular crack spacing, starting from the centre position for the first crack, where the tensile stress reaches the tensile strength, since the location of the first crack cannot be uniquely deduced from the stress field. An alternative scenario is that the cracks should arise simultaneously at several locations. Crack "simultaneous growing" in large mud slabs, forming a regularly spaced pattern of cracks within a short amount of time, is a common observation [17, 20].

Considering a material with homogeneously distributed flaws, a lower bound for the crack spacing should stem from the available energy to form cracks. Once the tensile strength is reached, energy conservation requires a portion of the elastic strain energy released due to crack formation to be converted into the surface energy of the cracks [7, 12, 30]. Using this concept, we derive hereafter an expression for the

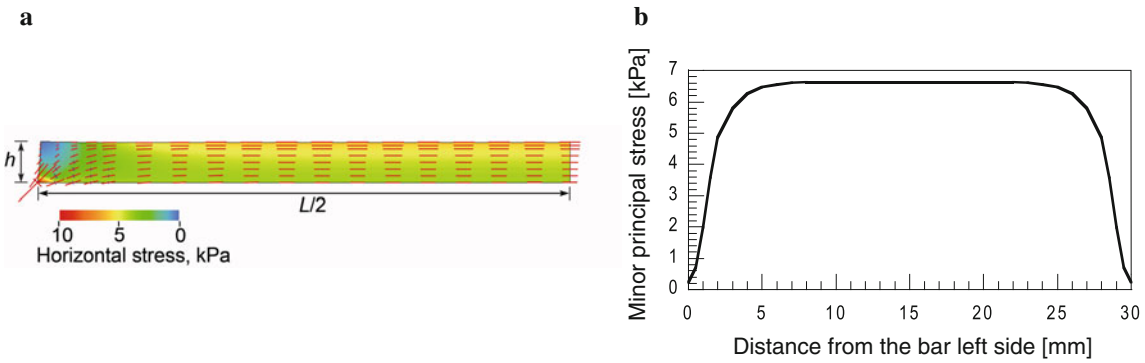

Fig. 4 Plane strain simulation of constrained desiccation tests. **a** Minor (tensile) principal stress field (*half bar*), onset of cracking: the lines stand for the orientation of the principal stresses (the length of the line is proportional to the stress absolute value); *red lines* are for tensile stresses, *blue lines* for compressive stresses; tensile stresses are taken as positive. **b** Minor principal stress profile along the bar top surface (same simulation as in **a**) (color figure online)

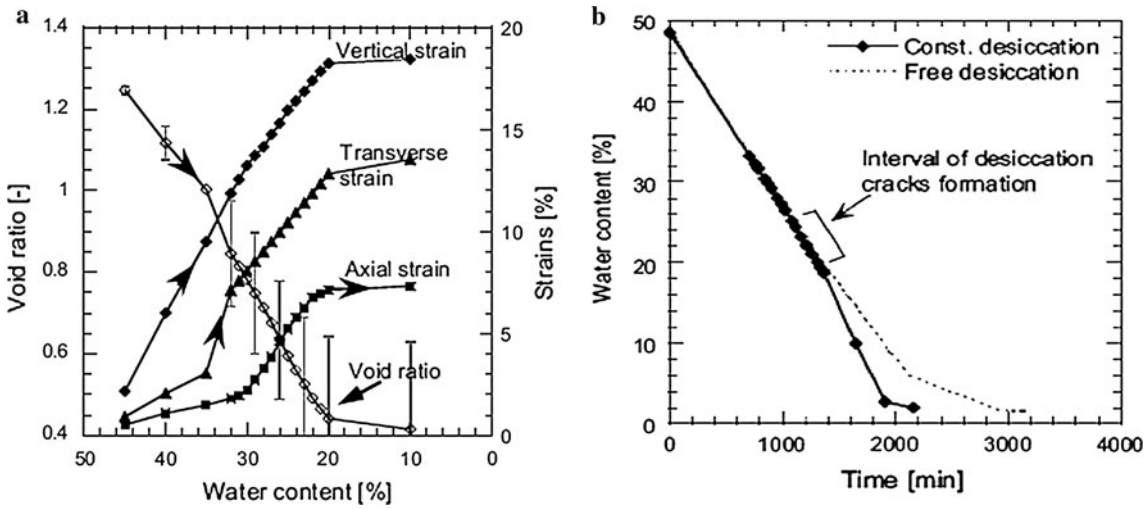

Fig. 5 **a** Strain and void ratio development during unconstrained drying, as compared to **b** the occurrence of the cracks in constrained drying. Cessation of straining and cracking takes place at nearly same water content, corresponding to the dewatering of the largest pores

crack spacing for a soil sample with a length L, width l and height h. The energy W_s required to form a system of N_C fully penetrating cracks is given by:

$$W_s = N_C h l \mathbf{G}_c \tag{1}$$

where $\mathbf{G}_c$ is the critical strain energy release rate, defined as the energy dissipated during fracture per unit of newly created fracture surface area. In the desiccation tests discussed here, it is reasonable to make a simplifying assumption that shrinkage is totally prevented in the axial direction, and totally free in the other directions, over the whole bar of soil. Furthermore, it is considered that all the elastic strain energy U is released during the process of cracking. Therefore,

$$U = ELhl\left(\varepsilon_x^{m,e}\right)^2 \Big/ 2 \tag{2}$$

where E is Young's modulus and $\varepsilon_x^{m,e}$ is the elastic part of the mechanical strain in the axial direction just before cracking. Setting W_s and U equal yields the number of cracks generated by one single energy release act:

$$N_C = (E/\mathbf{G}_c)L\left(\varepsilon_x^{m,e}\right)^2 \Big/ 2 \tag{3}$$

For the values of $\mathbf{G}_c$ reported for clay [4, 23], ranging from 0.2 N/m to 9 N/m, the crack spacing varies from 15 cm (i.e. 1 crack) to 0.8 cm (35 cracks), which is consistent with the average observed crack spacing obtained in our experiments.

The above energetic considerations provide a theoretical framework for the assessment of the formation of a crack pattern throughout a homogeneous stress field at a given level of drying. Upon further drying, the same concept applies, however, taking into account an axial stress relief due to the first generation of cracks and a subsequent cycle of the stress build-up upon a continuing shrinkage, up to the tensile stress reaching anew the tensile strength, at either several simultaneous several locations or, alternatively, following the sequential infilling process. The fragmentation process is not endless and a question arises: What are the mechanisms that control the final crack spacing? To explain why at a given moment cracking ceases and an ultimate spacing of cracks is attained ("fracture saturation" [6]), possible hypotheses include either the geometry of the drying body (spacing to thickness ratio [6]), on the basis of the already discussed sequential infilling process, or the mechanical boundary conditions [10] including interface delamination. They explain the desiccation cracking cessation by the fact that the stress field between two adjacent cracks does not reach in a consecutive reloading cycle the crack formation conditions (in terms of the tensile strength). However, no data on the local stress evolution near crack locations are available at present.

However, it needs to be reiterated that cracking is caused by an excess of the reaction-induced tensile stress, which in turn is proportional to the constrained shrinkage strain [24]. When the shrinkage dramatically decreases as a result of the air entry, further stressing change is minimal, as the water removal mechanism changes [14, 16]. Consistently, when shrinkage limit is reached, there is no further increase in the amount of energy available for cracking, since the increments of shrinkage strains and of the associated reactions tend to become zero from that time on. Indeed, it is seen from the results presented in Fig. 5 that the last crack is observed to form prior to the shrinkage limit.

For two-dimensional patterns, a similar principle can be adopted. For hexagonal patterns (i.e. the geometry that

minimizes surface energy consumption when tensile stress state in the plane perpendicular to the crack direction is isotropic), similar concepts as those developed above can be applied to the determination of the size of the hexagons. The other two-dimensional pattern limiting case (cracks intersecting at 90°) is straightforward since it results from successive one-dimensional crack pattern formations. Each generation of cracks aligns itself in the direction perpendicular to the local maximum tensile stress, that is, perpendicular to the existing cracks.

5 Conclusions

In conclusion, it is likely that the experimental crack patterns shown in Fig. 2d, e may result from a combination of the two processes discussed in this paper, "sequential infilling" or "simultaneous growing", since cracks in the experiments tended to appear either successively (at clearly decreasing overall water content values) or at the same time. This may well be the case for the two-dimensional case depicted in Fig. 1: a primary crack generation was first formed, the spacing of which can be explained by global considerations about the energy. Within the mud cells formed by the primary crack generation, the secondary crack generation would then stem from the evolved stress field. Actually, the "sequential infilling" concept for desiccation cracking should be invoked only when cells of an intact material with a reduced, well-defined size can be individualized.

Finally, eqs. (1–3) are valid also for the first crack in the infilling scenario, with the resulting $N_C = 1$, which leads to the conclusion that in such a case only a portion of the total accumulated energy is used to develop the single crack. That suggests that the unloading providing the energy for the first crack appearance is not complete, and the remaining $[(N_C - 1)/N_C]$-th of the accumulated energy at this point will contribute to the subsequent build-up of tensile stress up to the tensile strength value, and so forth for the next-generation cracks. Indeed, it must be re-emphasized that the result in eq. 3 is obtained under the assumption that the *entire* energy is consumed in generating all N_C cracks.

The answer to the question, which of the two scenarios will actually take place, is that it depends on whether or not there is any non-uniformity of the actual axial stress distribution resulting in a local maximum of it near the sample centre, or whether there are any imperfections in the kinematic constraints that would lead to the same kind of non-uniformity. Examples of a single crack appearing off-centre [25] confirm such interpretation. Simultaneous crack formation scenario is assumed to occur for a uniform stress distribution.

The interpretation proposed here provides a simplified but sound explanation and a tool to quantify the commonly observed crack spacing for a given pattern in soils. The controlling factor for the entire process of cracking is, in addition to Young's modulus, an experimentally determined critical strain energy release rate of a crack, which is considered in Linear Elasticity Fracture Mechanics to be a material characteristic.

Acknowledgments This work was funded by the Swiss National Science Foundation, grant # 200021_124702, and the US National Science Foundation, grant # 0324543. The authors would like to thank Anne Seibel for her contribution to the desiccation tests.

References

1. Albrecht BA, Benson CH (2001) Effect of desiccation on compacted natural clay. J Geotech Geoenviron Eng 127:67–75
2. Aubry D, Chouvet D, Modaressi A, Modaressi H (1995) Gefdyn: logiciel d'analyse du comportement mécanique des sols par éléments finis avec prise en compte du couplage sol-eau-air (Ecole Centrale Paris)
3. Irwin GR (1958) Fracture—Handbuch der Physik, vol 6. Springer, Berlin
4. Ayad R, Konrad JM, Soulié JM (1997) Desiccation of a sensitive day: application of the model CRACK. Can Geotech J 34: 943–951
5. Bai T, Pollard DD, Gao H (2000) Explanation for fracture spacing in layered materials. Nature 403:753–756
6. Bai T, Pollard DD, Gao H (2000) Spacing of edge fractures in layered materials. Int J Fract 103:373–395
7. Bazant ZP, Cedolin L (1991) Stability of structures—Elastic, inelastic, fracture, and damage theories, Ch. 12. Oxford University Press, Oxford
8. Bohn S, Platkiewicz J, Andreotti B, Adda-Bedia M, Couder Y (2005) Hierarchical crack pattern as formed by successive domain divisions. II. From disordered to deterministic behavior. Phys Rev E 71:046215
9. Coussy O (2004) Poromechanics. Chichester, UK
10. Groisman A, Kaplan E (1994) An experimental study of cracking induced by desiccation. Europhys Lett 25:415–420
11. Hillel D (1998) Environmental soil physics. Academic Press, San Diego
12. Hong AP, Li YN, Bazant ZP (1997) Theory of crack spacing in concrete pavement. J Eng Mech 123:267–275
13. Hu LB, Hueckel T, Peron H, Laloui L (2008) Desiccation shrinkage of unconstrained soil in the saturated phase. In: Proceeding 1st European conference on unsaturated soils, unsaturated soils: advances in geo-engineering, p 653–658
14. Hu LB, Peron H, Laloui L, Hueckel T (2011a) A multi-scale multi-physics model of soil drying. GeoFrontiers 2011, ASCE, GSP 211, p 4349–4359
15. Hu LB, Peron H, Laloui L, Hueckel T (2012a) Desiccation shrinkage of non-clayey soils: multi-physics mechanisms and a microstructural model. Int J Numer Anal Methods Geomech. doi: 10.1002/nag.2108
16. Hu LB, Peron H, Laloui L, Hueckel T (2012b) Desiccation shrinkage of non-clayey soils: a numerical study. Int J Numer Anal Methods Geomech. doi:10.1002/nag.2107
17. Konrad JM, Ayad R (1997) Desiccation of a sensitive clay: field experimental observations. Can Geotech J 34:929–942
18. Kowalski SJ (2003) Thermomechanics of drying processes. Springer, Berlin

19. Lachenbruch AH (1961) Depth and spacing of tension cracks. J Geophys Res 66:4273–4292
20. Miller CJ, Mi H, Yesiller N (1998) Experimental analysis of desiccation crack propagation in clay liners. J Am Water Resour Assoc 34:677–686
21. Morris PH, Graham J, Williams DJ (1992) Cracking in drying soils. Can Geotech J 29:262–277
22. Nahlawi N, Kodikara JK (2006) Laboratory experiments on desiccation cracking of thin soil layers. Geotech Geol Eng 24:1641–1664
23. Nichols JR, Grismer ME (1997) Measurement of fracture mechanics parameters in silty-clay soils. Soil Sci 162:309–322
24. Peron H, Hueckel T, Laloui L (2007) An improved volume measurement for determining soil water retention curve. Geotech Test J 30:1–8
25. Peron H, Hueckel T, Laloui L, Hu LB (2009) Fundamentals of desiccation cracking of fine-grained soils: experimental characterisation and mechanisms identification. Can Geotech J 46: 1177–1201
26. Peron H, Laloui L, Hueckel T, Hu LB (2009) Desiccation cracking of soils. Eur J Environ Civ Eng 13(7–8):869–888
27. Peron H, Laloui L, Hu LB, Hueckel T (2010) Desiccation of drying soils. In: Laloui L, Wiley J (eds) Mechanics of unsaturated geomaterials. Hoboken, NJ, pp 55–86
28. Ryan WBF, Major CO, Lericolais G, Goldstein SL (2003) Catastrophic flooding of the Black Sea. Annu Rev Earth Planet Sci 31:525–554
29. Scherer GW (1997) Stress from re-immersion of partially dried gel. J Non Cryst Solids 212:268–280
30. Thouless MD, Olsson E, Gupta A (1992) Cracking of brittle films on elastic substrates. Acta Metall Mater 40:1287–1292
31. Towner GD (1988) The influence of sand- and silt-size particles on the cracking during drying of small clay-dominated aggregates. J Soil Sci 39:347–356